Neoclassical transport coefficients for general axisymmetric equilibria in the banana regime

C. Angioni[a] and O. Sauter
Centre de Recherches en Physique des Plasmas, Association EURATOM-Confédération Suisse, Ecole Polytechnique Fédérale de Lausanne, 1015 Lausanne, Switzerland

(Received 6 October 1999; accepted 3 January 2000)

Using the standard approach of neoclassical theory, a set of relatively simple kinetic equations has been obtained, suited for an implementation in a numerical code to compute a related set of distribution functions. The transport coefficients are then expressed by simple integrals of these functions and they can be easily computed numerically. The code CQL3D [R. W. Harvey and M. G. McCoy, in *Proceedings of IAEA Technical Committee Meeting on Advances in Simulation and Modeling of Thermonuclear Plasmas, Montreal, 1992* (International Atomic Energy Agency, Vienna, 1993), pp. 489–526], which uses the full collision operator and considers the realistic axisymmetric configuration of the magnetic surfaces, has been modified to solve the bounce-averaged version of these equations. The coefficients have then been computed for a wide variety of equilibrium parameters, high-lighting interesting features of the influence of geometry at small aspect ratio. Differences with the most recent formulas for the ion neoclassical heat conductivity are pointed out. A set of formulas, which fit the code results, is obtained to easily evaluate all the neoclassical transport coefficients in the banana regime, at all aspect ratios, in general axisymmetric equilibria. This work extends to all the other transport coefficients, at least in the banana regime, the work of Sauter *et al.* [O. Sauter, C. Angioni, and Y. R. Lin-Liu, Phys. Plasmas **6**, 2834 (1999)] which evaluates the neoclassical conductivity and all the bootstrap current coefficients. Formulas for arbitrary collisionality regime are proposed, obtained combining our results for the banana regime with the results of Hinton and Hazeltine [F. L. Hinton and R. D. Hazeltine, Rev. Mod. Phys. **48**, 239 (1976)], adapted for small aspect ratio. © *2000 American Institute of Physics.* [S1070-664X(00)02404-6]

I. INTRODUCTION

Recent improvements in neoclassical transport theory are almost completely dedicated to parallel transport. In particular, in Ref. 2, we have computed the neoclassical conductivity and all the bootstrap current coefficients, taking into account the full collision operator and including the advection parallel to the magnetic field, considering the realistic axisymmetric magnetic configuration of the flux surface. We have given relatively simple formulas valid for general axisymmetric equilibria and arbitrary collisionality regimes. For the other transport coefficients, improvements have been done only on the ion thermal conductivity in the banana regime[4–6] and for various collision frequencies.[7] Important recent new results have been presented in Ref. 8, solving a set of multispecies fluid equations: this enables one to compute the neoclassical conductivity, the bootstrap current and the particle and heat neoclassical fluxes, for arbitrary collisionality and aspect ratio. However, a set of equations must be solved in a specific code, which is not practically suited for numerical implementation in one-dimensional tokamak transport modelling codes. Moreover, all these latter results[4–8] use an approximate collision operator, usually following the expansion method of Hirshman and Sigmar.[9] This method was also used to compute the like–particle collisions contribution on the viscosity matrix,[4] and these results were applied in Ref. 10 to compute the bootstrap current coefficients at low aspect ratio. When compared with Ref. 2, these results are in very good agreement in general, but present a non-negligible error on the bootstrap current coefficients in which the contribution given by the like–particle collision operator is particularly important.[2] For all the electron perpendicular transport coefficients the only formulas available at small aspect ratio are those in Ref. 11, valid in the banana regime, which use the analytical values of the transport coefficients at $\epsilon = 1$ and the values at large aspect ratio of Ref. 12 to obtain a set of formulas with a linear interpolation between these two limits, which should be valid also at small aspect ratio. In the more recent investigations on the ion thermal conductivity,[5,6] the intermediate aspect ratio corrections show a difference with the results of Ref. 11 of almost a factor of 2. In this sense a complete investigation of the small aspect ratio corrections for all the neoclassical transport coefficients, taking into account the full collision operator, is necessary. It is well known that the neoclassical theory can not completely explain the perpendicular transport in tokamaks, however a precise computation is useful in order to allow a correct evaluation of the anomalous contribution by means of the comparison with the experimental data. This is becoming even more important with the recent improved

[a]Author to whom correspondence should be addressed. Electronic mail: Clemente.Angioni@epfl.ch

confinement modes of operation, with internal transport barriers and relatively small anomalous transport.

In Sec. II we describe the approach to obtain the linear drift-kinetic equations suitable for implementation in a Fokker–Planck code and the expressions to compute the transport coefficient as simple integrals of the distribution functions. The related bounce-averaged equations in the banana regime are then obtained, and the Lorentz model is investigated analytically. In Sec. III we show the numerical results for the banana regime, computed with the Fokker–Planck code CQL3D,[1] which solves the linearized drift kinetic bounce-averaged equation with the full collision operator and considering the realistic axisymmetric configuration of the magnetic surfaces. Some benchmarks are considered to validate the results, and the comparison with some previous numerical and analytical results is shown. In Sec. IV we give a set of formulas which fit our numerical results and allow to easily evaluate all the neoclassical transport coefficients in general axisymmetric equilibria for arbitrary aspect ratio and ion charge in the banana regime. Combined formulas for arbitrary collisionality regime are then proposed in the last subsection.

II. KINETIC THEORY

A. Transport coefficients

Our approach follows the standard neoclassical theory, in particular the one of Ref. 3. The flux surface averaged thermodynamic forces and their conjugated neoclassical fluxes are chosen as follows:

$$\begin{pmatrix} \Gamma_e \dfrac{d\psi}{d\rho} \\ \dfrac{Q_e}{T_e}\dfrac{d\psi}{d\rho} \\ \left\langle \dfrac{j_\parallel B}{T_e}\right\rangle - \left\langle \dfrac{j_{\parallel S} B}{T_e}\right\rangle \\ -\dfrac{I(\psi)\langle E_* B\rangle n_e}{\langle B^2\rangle} \end{pmatrix} = \begin{bmatrix} \mathcal{L}^e_{11} & \mathcal{L}^e_{12} & \mathcal{L}^e_{13} & \mathcal{L}^e_{14} \\ \mathcal{L}^e_{21} & \mathcal{L}^e_{22} & \mathcal{L}^e_{23} & \mathcal{L}^e_{24} \\ \mathcal{L}^e_{31} & \mathcal{L}^e_{32} & \mathcal{L}^e_{33} & \mathcal{L}^e_{34} \\ \mathcal{L}^e_{41} & \mathcal{L}^e_{42} & \mathcal{L}^e_{43} & \mathcal{L}^e_{44} \end{bmatrix} \times \begin{pmatrix} \dfrac{1}{p_e}\dfrac{\partial p_e}{\partial \psi} + \dfrac{1}{p_e}\dfrac{\partial p_i}{\partial \psi} \\ \dfrac{1}{T_e}\dfrac{\partial T_e}{\partial \psi} \\ \dfrac{\langle E_\parallel B\rangle}{\langle B^2\rangle} \\ \dfrac{q_e}{n_i T_e}\dfrac{K_i(\psi)}{I(\psi)}\langle B^2\rangle \end{pmatrix}, \tag{1a}$$

$$\begin{pmatrix} \dfrac{\langle j_{\parallel Ri} B\rangle}{T_i} \\ \dfrac{Q_i}{T_i}\dfrac{d\psi}{d\rho} \end{pmatrix} = \begin{bmatrix} \mathcal{L}^i_{11} & \mathcal{L}^i_{12} \\ \mathcal{L}^i_{21} & \mathcal{L}^i_{22} \end{bmatrix} \begin{pmatrix} -\dfrac{\langle E_* B\rangle}{\langle B^2\rangle} \\ \dfrac{1}{T_i}\dfrac{\partial T_i}{\partial \psi} \end{pmatrix}. \tag{1b}$$

The right-hand side vectors of Eqs. (1a) and (1b) are, respectively, the electron and ion forces, which will be referred as A_{en} and A_{in} and the left-hand side vectors are their conjugated neoclassical fluxes, referred as B_{en} and B_{in}. Γ_σ and Q_σ are the particle and heat fluxes of species σ, $j_\parallel$ is the total parallel electric current, $j_{\parallel S}$ is the Spitzer current, $j_{\parallel Ri}$ is the ion contribution to the so-called ''return current,'' $E_* \doteq E_\parallel + F_{i\parallel}(q_i n_i)^{-1}$ is the ''effective electric field'' and $F_{i\parallel}$ is the friction force between ions and electrons. We have called ρ a generic radial coordinate and $\langle\,\rangle$ denotes the flux surface average. The function $K_i(\psi)$, of the magnetic poloidal flux ψ, is related to the flux surface average $\langle j_{\parallel Ri} B\rangle$ by the equation: $\langle j_{\parallel Ri} B\rangle = q_i K_i(\psi)\langle B^2\rangle$. Note that ion and electron forces and fluxes are mutually dependent

$$B_{i1} = -I(\psi) n_e \frac{T_e}{T_i} A_{e4}, \quad B_{e4} = I(\psi) n_e A_{i1}. \tag{2}$$

The kinetic expressions of the conjugated neoclassical thermodynamic fluxes can be written in the following form:

$$B_{en} = \left\langle \int d\mathbf{v} (v_\parallel \hat{\mathbf{b}}\cdot\nabla\gamma_{en}) \left(G_e - \sum_n \gamma_{en} A_{en} f_{e0}\right)\right\rangle, \quad n = 1,2,3,4, \tag{3}$$

$$B_{in} = \left\langle \int d\mathbf{v} \beta_{in} (G_i - \gamma_{i2} A_{i2} f_{i0})\right\rangle, \quad n = 1,2, \tag{4}$$

in which we have introduced the functions

$$\gamma_{e1} = \frac{I(\psi) v_\parallel}{\Omega_e}, \quad \gamma_{e2} = \gamma_{e1}\left(\frac{v^2}{v_{Te}^2} - \frac{5}{2}\right),$$

$$\gamma_{e3} = \frac{v_\parallel f_{se}}{f_{e0}} B, \quad \gamma_{e4} = \gamma_{e1}\frac{B^2}{\langle B^2\rangle},$$

$$\beta_{i1} = \frac{q_i v_\parallel}{T_i} B, \quad \beta_{i2} = v_\parallel \hat{\mathbf{b}}\cdot\nabla(\gamma_{i2}),$$

$$\gamma_{i2} = \frac{I(\psi) v_\parallel}{\Omega_i}\left(\frac{v^2}{v_{Ti}^2} - \frac{5}{2}\right).$$

The distribution functions G_e and G_i are related to the first-order perturbations, f_{e1} and f_{i1}, by means of two suitable transformations. The first one follows Eqs. (5.42) and (5.43) of Ref. 3, leading to the functions H_e and H_i. Then the second one, simply $G_e = H_e + \Sigma_n \gamma_{en} A_{en} f_{e0}$ and $G_i = H_i + \gamma_{i2} A_{i2} f_{i0}$, allows to write the Linearized Drift Kinetic Fokker–Planck equations, Ref. 3, Eqs. (5.21)–(5.24), in the following simple form:

$$v_\parallel \hat{\mathbf{b}}\cdot\nabla G_e - C^l_{e0}(G_e) = -\sum_n C^l_{e0}(\gamma_{en} f_{e0}) A_{en}, \tag{5}$$

$$v_\parallel \hat{\mathbf{b}}\cdot\nabla G_i - C^l_{ii}(G_i) = -\beta_{i1} f_{i0} A_{i1} - C^l_{ii}(\gamma_{i2} f_{i0}) A_{i2}, \tag{6}$$

in which the collision operators C^l_{e0} and C^l_{ii} are, respectively, defined in Eqs. (4.45) and (1.19) of Ref. 3. Note that these equations are particularly useful, as all the coefficients of the thermodynamic forces in the source terms can be evaluated analytically[13]

$$-C^l_{e0}(\gamma_{e1} f_{e0}) = Z_i \nu_{e0}(v)\gamma_{e1} f_{e0},$$

$$-C^l_{e0}(\gamma_{e2}f_{e0}) = Z_i\nu_{e0}(v)\gamma_{e2}f_{e0} - \nu_{e0}(v)h\left(\frac{v}{v_{Te}}\right)\gamma_{e1}f_{e0},$$

$$-C^l_{e0}(\gamma_{e3}f_{e0}) = \frac{q_e v_\parallel B}{T_e}f_{e0}, \tag{7}$$

$$-C^l_{e0}(\gamma_{e4}f_{e0}) = Z_i\nu_{e0}(v)\gamma_{e4}f_{e0},$$

$$-C^l_{ii}(\gamma_{i2}f_{e0}) = -\nu_{i0}(v)h\left(\frac{v}{v_{Ti}}\right)\frac{I(\psi)v_\parallel}{\Omega_i}f_{i0},$$

with

$$\nu_{e0}(v) = \frac{\nu_{ei}(v)}{Z} = \frac{3\sqrt{\pi}v_{Te}^3}{4Z_i\tau_e v^3}, \quad \nu_{i0}(v) = \frac{3\sqrt{\pi}v_{Ti}^3}{2\sqrt{2}\tau_i v^3},$$

$$h(x) = (10-4x^2)\mathrm{erf}(x) - 10x\,\mathrm{erf}'(x),$$

and, according to definitions given in Ref. 3

$$\frac{1}{\tau_e} = \frac{4}{3}\sqrt{2\pi}\frac{n_i e^4\ln\Lambda}{m_e^{1/2}T_e^{3/2}}, \quad \frac{1}{\tau_i} = \frac{4}{3}\sqrt{\pi}\frac{n_i Z_i^4 e^4\ln\Lambda}{m_i^{1/2}T_i^{3/2}}. \tag{8}$$

Introducing the set of functions $g_{\sigma n}$, in such a way that $G_\sigma = \Sigma_n g_{\sigma n}A_{\sigma n}$, Eqs. (5) and (6) can be linearly decoupled

$$v_\parallel\hat{\mathbf{b}}\cdot\nabla g_{en} - C^l_{e0}(g_{en}) = -C^l_{e0}(\gamma_{en}f_{e0}), \quad n=1,2,3,4. \tag{9}$$

$$v_\parallel\hat{\mathbf{b}}\cdot\nabla g_{i1} - C^l_{ii}(g_{i1}) = -\beta_{i1}f_{i0}, \tag{10a}$$

$$v_\parallel\hat{\mathbf{b}}\cdot\nabla g_{i2} - C^l_{ii}(g_{i2}) = -C^l_{ii}(\gamma_{i2}f_{i0}). \tag{10b}$$

The kinetic definitions of the thermodynamic fluxes, Eqs. (3) and (4), written in terms of the functions $g_{\sigma n}$, allow to readily identify the transport coefficients, introduced in Eq. (1)

$$\mathcal{L}^e_{mn} = \left\langle \int d\mathbf{v}\gamma_{em}C^l_{e0}(\gamma_{en}f_{e0})\right\rangle - \left\langle \int d\mathbf{v}\frac{g_{em}}{f_{e0}}C^l_{e0}(\gamma_{en}f_{e0})\right\rangle, \quad n,m=1,2,3,4, \tag{11}$$

$$\mathcal{L}^i_{1n} = \left\langle \int d\mathbf{v}g_{in}\beta_{i1}\right\rangle, \quad n=1,2,$$

$$\mathcal{L}^i_{21} = -\left\langle \int d\mathbf{v}\frac{g_{i1}}{f_{i0}}C^l_{ii}(\gamma_{i2}f_{i0})\right\rangle, \tag{12}$$

$$\mathcal{L}^i_{22} = \left\langle \int d\mathbf{v}\gamma_{i2}C^l_{ii}(\gamma_{i2}f_{i0})\right\rangle - \left\langle \int d\mathbf{v}\frac{g_{i2}}{f_{i0}}C^l_{ii}(\gamma_{i2}f_{i0})\right\rangle.$$

In this way we have obtained a simple set of expressions to compute all the neoclassical transport coefficients, once we have solved the drift-kinetic equations, Eqs. (9) and (10), to obtain the distribution functions g_{en} and g_{in}. We see that every expression is composed of the sum of two terms: The first one is an integral that can be computed analytically and that, for some coefficients, is identically zero; the second one has an integrand in which the only term to be computed numerically is the distribution function g_{en} or g_{in}. Note that in the banana regime the first term, computed analytically, gives directly the value of the transport coefficient at $\epsilon=1$, when all the particles are trapped; the second term gives the reduction of transport due to the presence of passing particles. In Appendix A we show that Eqs. (11) and (12) satisfy the Onsager relations of symmetry as expected.

B. Banana regime: bounce-averaged equations

When the collision frequency ν_{ei} is much smaller than the bounce frequency ν_b, the distribution functions g_{en} can be expanded as follows:

$$g_{en} = g^0_{en} + \left(\frac{\nu_{ei}}{\nu_b}\right)g^1_{en} + O\left[\left(\frac{\nu_{ei}}{\nu_b}\right)^2\right],$$

and analogously for the ion distribution functions. A somewhat standard derivation[3,12] shows that the functions $g^0_{\sigma n}$ are independent of the poloidal angle θ_p, and that they are zero in the trapped particle region of velocity space. In the passing particle region, the functions $g^0_{\sigma n}$ satisfy the following bounce-averaged equations:

$$\int_{-\pi}^{\pi} d\theta_p \frac{B}{|v_\parallel|}C^l_{e0}(g^0_{en}) = S_{en}, \quad n=1,2,3,4, \tag{13a}$$

$$\int_{-\pi}^{\pi} d\theta_p \frac{B}{|v_\parallel|}C^l_{ii}(g^0_{in}) = S_{in}, \quad n=1,2, \tag{13b}$$

with

$$S_{en} \doteq 2\pi\sigma\langle BC^\gamma_{en}(v,B)\rangle f_{e0}, \quad n=1,2,3,4, \tag{13c}$$

$$S_{i1} \doteq 2\pi\sigma\frac{q_i\langle B^2\rangle}{T_i}f_{i0}, \quad S_{i2} \doteq 2\pi\sigma\langle BC^\gamma_{i2}(v,B)\rangle f_{i0}, \tag{13d}$$

where $\sigma = v_\parallel/|v_\parallel|$ and where we have introduced the set of functions $\mathcal{C}^\gamma_{\sigma n}(v,B)$, defined as follows:

$$\mathcal{C}^\gamma_{\sigma n}(v,B) \doteq C^l_\sigma(\gamma_{\sigma n}f_{\sigma 0})/(v_\parallel f_{\sigma 0}).$$

The analytical expressions of these functions can easily be obtained from Eqs. (7). Note that $\langle BC^\gamma_{e4}(v,B)\rangle = \langle BC^\gamma_{e1}(v,B)\rangle$, so that the functions g^0_{e1} and g^0_{e4} solve the same equation in the banana regime; in particular it follows that $\mathcal{L}_{44} = \mathcal{L}_{14}$: This is a consequence of our choice of thermodynamic forces and fluxes. We see that at $\epsilon=1$, when all the particles are trapped, the distribution functions g^0_{en} are zero everywhere, and the first terms in the expressions for the transport coefficients, Eqs. (11) and (12), give directly the entire coefficient. The code CQL3D has been modified to solve Eqs. (13) in general axisymmetric equilibria and with the full collision operator.

C. Lorentz model

For the Lorentz gas model, $Z_i \gg 1$, the set of Eqs. (13a) is solved analytically.[3,14] In fact, as collisions between electrons can be neglected, the collision operator can be approximated by the pitch-angle scattering operator:

$$C^l_{e0}=\nu_{ei}(v)L\doteq\nu_{ei}(v)\,\frac{1}{2}\,\frac{\partial}{\partial\xi}(1-\xi^2)\,\frac{\partial}{\partial\xi}\quad\text{and}\quad\xi\doteq\frac{v_\parallel}{v}.$$

The solutions of Eq. (13a) in this approximation can be written in the following form:

$$g^0_{en}=-\sigma\,\frac{v}{2\,\nu_{ei}(v)}\langle BC^\gamma_{en}(v,B)\rangle f_{e0}\times\int_\lambda^{\lambda_c}\frac{d\lambda'}{\langle(1-\lambda' B)^{1/2}\rangle}H(\lambda_c-\lambda),\tag{14}$$

where $\lambda\doteq(1-\xi^2)/B$, $\lambda_c\doteq 1/B_{\max}$ and $H(x)$ is the Heaviside function. Introducing Eq. (14) in the expressions for the coefficients Eqs. (11), all the electron transport coefficients can be written as integrals in the absolute value of velocity v

$$\mathcal{L}^e_{mn}=\frac{4\pi}{3}\int_0^\infty v^4dv\left\langle\frac{\gamma_{em}}{v_\parallel}C^\gamma_{en}\right\rangle f_{e0}+\pi\int_0^\infty\frac{v^4dv}{\nu_{ei}(v)}\langle BC^\gamma_{em}\rangle\times\langle BC^\gamma_{en}\rangle f_{e0},\quad n,m=1,2,3,4.$$

The integrals of v can easily be computed analytically, and the results have been compared with Ref. 3, Eqs. (5.121), (5.124)–(5.130), finding a complete agreement. As the Lorentz model coefficients will be used not only as a benchmark for the results of CQL3D, but also to analyze the results of the code with the full collision operator and in different axisymmetric configurations, we report all the electron transport coefficients, which can be written in the following simple form:

$$\mathcal{L}^e_{11}=-0.5\mathcal{L}_d[B_0^2\langle B^{-2}\rangle]f_t^d,\tag{15a}$$

$$\mathcal{L}^e_{21}=0.75\mathcal{L}_d[B_0^2\langle B^{-2}\rangle]f_t^d,\qquad\mathcal{L}^e_{22}=-\tfrac{13}{8}\mathcal{L}_d[B_0^2\langle B^{-2}\rangle]f_t^d,\tag{15b}$$

$$\mathcal{L}^e_{31}=\mathcal{L}^e_{34}=-\mathcal{L}_b f_t,\quad\mathcal{L}^e_{32}=0,\qquad\mathcal{L}^e_{33}=-\frac{32}{3\pi}\mathcal{L}_\sigma[B_0^{-2}\langle B^2\rangle]f_t,\tag{15c}$$

$$\mathcal{L}^e_{41}=\mathcal{L}^e_{44}=-0.5\mathcal{L}_d[B_0^2\langle B^2\rangle^{-1}]f_t,\qquad\mathcal{L}^e_{42}=0.75\mathcal{L}_d[B_0^2\langle B^2\rangle^{-1}]f_t.\tag{15d}$$

with

$$\mathcal{L}_d=\frac{n_e\rho^2_{ep}}{\tau_e}\left(\frac{d\psi}{d\rho}\right)^2,\quad\mathcal{L}_b=I(\psi)n_e,\quad\mathcal{L}_\sigma=\frac{n_eq_e^2\tau_e}{m_eT_e}B_0^2,\tag{16}$$

and where we have introduced two definitions for the trapped fraction

$$f_t^d=1-\tfrac{3}{4}\langle B^{-2}\rangle^{-1}\mathcal{I}_\lambda,\quad f_t=1-\tfrac{3}{4}\langle B^2\rangle\mathcal{I}_\lambda,\qquad\mathcal{I}_\lambda=\int_0^{\lambda_c}\frac{\lambda'd\lambda'}{\langle(1-\lambda' B)^{1/2}\rangle}.\tag{17}$$

The second one, f_t, is the usual definition for the trapped particle fraction.[4] Note that the integral $\mathcal{I}_\lambda$ can easily be evaluated using the formulas in Ref. 15. The poloidal gyroradius $\rho_{\sigma p}$ of species σ is given by

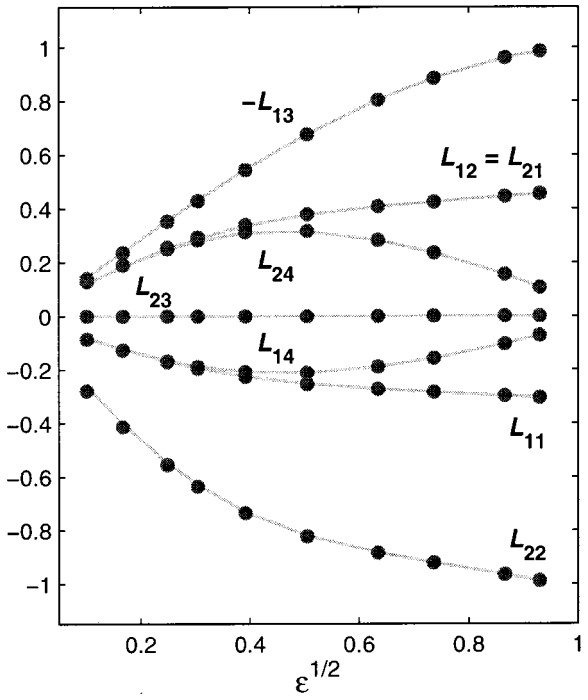

FIG. 1. Transport coefficients $\mathcal{L}^e_{1n}$ and $\mathcal{L}^e_{2n}$ for an almost cylindrical equilibrium, computed by CQL3D in the approximation of the Lorentz model (circles), and compared with the analytical results, Eq. (15).

$$\rho_{\sigma p}(\rho)=\frac{v_{T\sigma}}{|\Omega_{\sigma p}|}=\frac{\sqrt{2m_\sigma T_\sigma}}{|q_\sigma|B_{p0}(\rho)},\tag{18}$$

like in Ref. 3, Eq. (5.122), where the poloidal magnetic field $B_{po}(\rho)$ is defined by $B_{po}\doteq(d\psi/d\rho)B_0(\psi)/I(\psi)$, and $B_0(\psi)$ is an arbitrarily chosen function introduced to normalize the magnetic field on a given flux surface. Note that the flux surface averaged integrals I_{11}, I_{13}, and I_{33} which appear in the results of Ref. 3 can be reduced to only the two trapped fractions, Eq. (17), with the following relations:

$$I_{11}=\tfrac{4}{3}[B_0^2\langle B^{-2}\rangle]f_t^d,\quad I_{13}=\tfrac{4}{3}f_t,\quad I_{33}=\tfrac{4}{3}[B_0^{-2}\langle B^2\rangle]f_t.\tag{19}$$

We see, therefore, that all the coefficients in the Lorentz model depend essentially on f_t^d and f_t. We shall show in the next Sections that in the general case this property remains true, namely that all the equilibrium effects on the neoclassical transport coefficients are functions of only these two trapped fractions.

III. NUMERICAL RESULTS

A. Benchmarks

As the Lorentz model gives an analytical solution, it can be used as a first benchmark for the numerical results. In Fig. 1 we show the transport coefficients $\mathcal{L}^e_{1n}$ and $\mathcal{L}^e_{2n}$ relative to the sources S_{e1} and S_{e2}, Eqs. (13), computed by CQL3D in the approximation of the Lorentz model: very good agreement is obtained for all ϵ. The coefficients in the Figure, indicated by L^e_{mn}, are plotted normalized by the relative factors $\mathcal{L}_d$ or $\mathcal{L}_b$ given in Eq. (16). This normalization for the electron transport coefficients is also kept in Figs. 2 and 4,

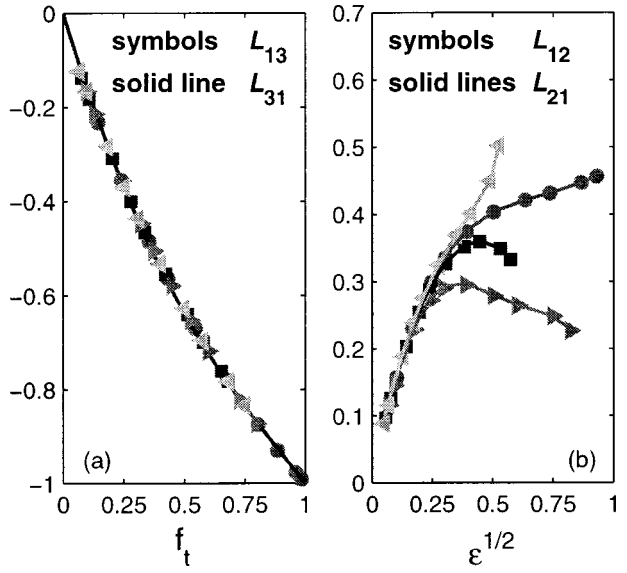

FIG. 2. Onsager symmetry is correctly respected by the numerical results. (a) The transport coefficient $\mathcal{L}^e_{13}$ (symbols), plotted vs f_t, is well aligned with the formula (14a) of Ref. 1 for the bootstrap current coefficient $\mathcal{L}^e_{31}$ (solid line). The different symbols refer to different equilibria in all the figures. Note that the results given by the different equilibria are perfectly overlapped, as they are plotted vs f_t. (b) Transport coefficient $\mathcal{L}^e_{12}$ (symbols) and $\mathcal{L}^e_{12}$ (solid lines) computed with four different equilibria, plotted vs $\epsilon^{1/2}$. Note that when the complete coefficients are plotted vs the inverse aspect ratio, a strong dependence on equilibria appears at small aspect ratio.

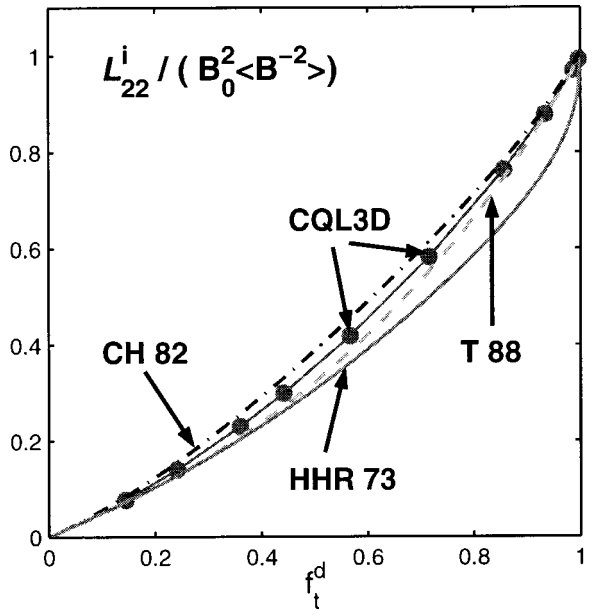

FIG. 3. The ion heat conductivity, transport coefficient $\mathcal{L}^i_{22}$, computed by CQL3D with an almost cylindrical equilibrium (solid circles), divided by the flux surface average $B^2_0\langle B^{-2}\rangle$, plotted vs the trapped particle fraction f^d_t and compared with formulas of Ref. 3, CH 82 (dashed–dotted line), Ref. 4, T 88 (dashed line), and Ref. 9 (modified), HHR 73 (solid line).

and analogously in Fig. 3 for the ion transport coefficients. The complete definition of a set of dimensionless coefficients will be given in the next section.

When the full collision operator is used, the symmetry of the transport matrix gives a second benchmark of the numerical results: indeed, each off-diagonal coefficient can be computed in two different ways, $\mathcal{L}_{nm}$ and $\mathcal{L}_{mn}$. Note that we have already computed[2] the neoclassical resistivity and the bootstrap current coefficients $\mathcal{L}_{3n}$, $n=1,2,4$. In Fig. 2(a) we plot the results for the coefficient $\mathcal{L}^e_{13}$, computed solving the kinetic equation with the source S_{e1}, Eqs. (13a) and (13c), $n=1$: they are perfectly aligned with the solid line given by Eq. (14a) of Ref. 2, which fits the code results for the bootstrap current coefficient $\mathcal{L}^e_{31}$, hence computed with the source S_{e3}, Eqs. (13a) and (13c), $n=3$. The exact relations between the bootstrap current coefficients defined in Ref. 2 and the transport coefficients defined in this paper will be presented in the next section. In Fig. 2(b) we plot the two coefficients $\mathcal{L}^e_{12}$ and $\mathcal{L}^e_{21}$, computed considering four different equilibria, as shown in Fig. 1 of Ref. 2, and whose main specifications and related symbols, full or open, used in all the figures, are given in Table I. The coefficient $\mathcal{L}^e_{12}$, obtained solving Eqs. (13a) and (13c), $n=1$, is plotted with symbols, the coefficient $\mathcal{L}^e_{21}$, obtained solving Eqs. (13a) and (13c), $n=2$, is plotted with solid lines: we find a very good agreement between the two coefficients, within 1% for $\epsilon \geqslant 0.1$. We see also that the behavior of the transport coefficient strongly depends on the equilibrium at small aspect ratio. Previous formulas, which give the transport coefficients with an expansion in powers of $\epsilon^{1/2}$, are correct only for almost cylindrical equilibria and are of practical interest in general equilibria only for $\epsilon<0.1$: this must be taken into account when comparing with our results. It indicates that for each transport coefficient an appropriate geometrical parameter, like f_t for $\mathcal{L}^e_{31}$ and $\mathcal{L}^e_{13}$ in Fig. 2(a), needs to be used instead of ϵ, as it will be shown in the next subsection.

TABLE I. Equilibria specifications and related symbols used in the figures.

Symbol	R_{mag} [m]	R_{geo} [m]	a [m]	k	δ
○	2.13	2.13	1.925	1.0	0
□	8.44	8.00	2.750	1.8	0.32
▷	1.67	1.22	0.875	3.0	0.56
◁	0.92	0.88	0.252	2.5	−0.65

B. Comparison with previous results and behavior at small aspect ratio

As we have said in Sec. I, the most recent investigations on perpendicular neoclassical transport were dedicated only to the ion thermal conductivity.[5,6] In Fig. 3 we compare our results for the coefficient $\mathcal{L}^i_{22}$, obtained with an almost cylindrical equilibrium, with the results of Refs. 5, 6, and 11. As mentioned at the end of the previous paragraph, a correct geometrical parameter must be chosen to plot a given transport coefficient. As it can be inferred from the Lorentz model results for the electron coefficient $\mathcal{L}^e_{22}$, Eq. (15b), and as it will be presented later, the ion heat conductivity is a function of the trapped fraction f^d_t, Eq. (17). We find good agreement with the most recent formulas of Refs. 5 and 6. These results enable to finally resolve the discrepancy between the formulas given in Refs. 5 and 6, obtained with approximated collision operators. It turns out that the results with the full collision operator, CQL3D, are in between the previous re-

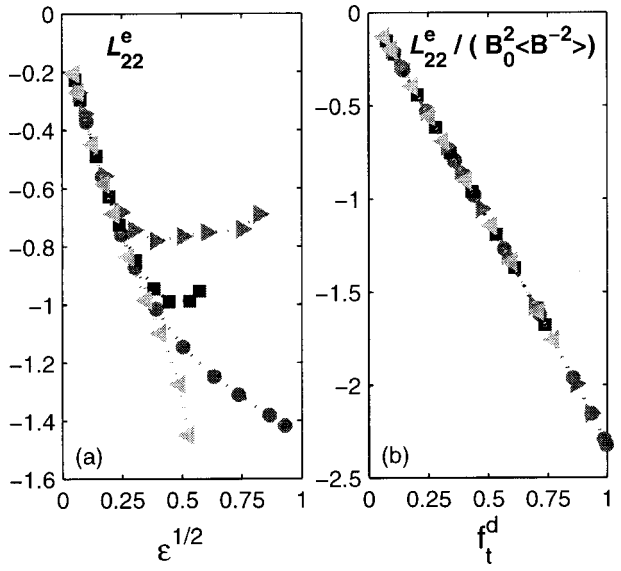

FIG. 4. The transport coefficient $\mathcal{L}^e_{22}$, main contribution to the electron heat conductivity, computed by CQL3D with four different equilibria: (a) The complete coefficient is plotted vs $\epsilon^{1/2}$, a strong dependence on the different equilibria appears at small aspect ratio; (b) the coefficient is divided by an appropriate flux surface average $B_0^2\langle B^{-2}\rangle$, and plotted vs the correct geometrical parameter, f_t^d, which allows to perfectly align all the points of the different equilibria.

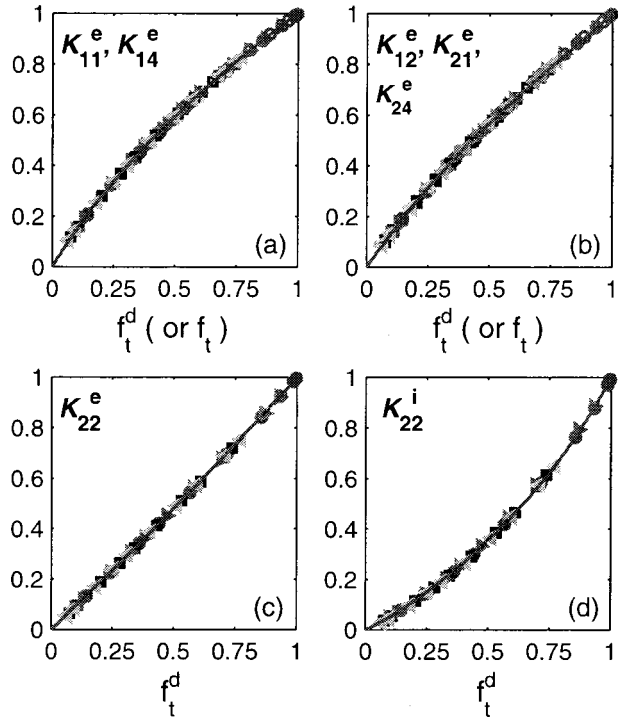

FIG. 5. Computed values of the dimensionless transport coefficients $\mathcal{K}^\sigma_{mn}$ (symbols), compared with the fitting formulas, Eqs. (23) and (24) (solid lines). (a) Coefficients $\mathcal{K}^e_{11}$ plotted vs f_t^d (solid symbols), and $\mathcal{K}^e_{14}$ plotted vs f_t (open symbols). (b) Coefficients $\mathcal{K}^e_{12}$ and $\mathcal{K}^e_{21}$, plotted vs f_t^d (solid symbols), and $\mathcal{K}^e_{24}$ plotted vs f_t (open symbols). (c) Coefficient $\mathcal{K}^e_{22}$ plotted vs f_t^d (solid symbols). (d) Coefficient $\mathcal{K}^i_{22}$ plotted vs f_t^d (solid symbols).

sults. Note that the plotted formula of Ref. 11 has been modified, keeping in the expression for the transport coefficient the flux surface average of the magnetic field, which were correctly computed in the reference to obtain the limit at $\epsilon=1$, but then not taken into account in the final formulas.

When different axisymmetric equilibria are considered in the numerical calculations, the transport coefficients present particular features of the influence of geometry at small aspect ratio, as already highlighted in Fig. 2(b). In Fig. 4 we also show the electron coefficient $\mathcal{L}^e_{22}$, computed with the four different equilibria of Table I. In Fig. 4(a), $\mathcal{L}^e_{22}$ is plotted versus $\epsilon^{1/2}$: we see differences up to 30% already at $\epsilon=0.15$. In Fig. 4(b) we show the same coefficient $\mathcal{L}^e_{22}$ divided by the flux surface average $(B_0^2\langle B^{-2}\rangle)$ and plotted versus the trapped particle fraction f_t^d, defined in Eq. (17), as suggested by the results of the Lorentz model: the points are well-aligned at all f_t^d, i.e., at all ϵ. The same behavior is obtained for all the other transport coefficients: the coefficients must be normalized by a suitable flux surface average and a correct geometrical parameter must be used to encapsulate the effects of the different equilibria. Note that the definition of a new trapped particle fraction, f_t^d, Eq. (17), is effectively necessary, as suggested by the Lorentz model, to correctly describe the geometrical behavior of certain coefficients, in particular all the particle and heat conductivities, for which the usual one, f_t, turns out to be inadequate. From Fig. 4 it is also evident that, when plotted versus the correct parameter, the transport coefficients turn out to be very simple functions, almost proportional to the appropriate trapped fraction. This explains the relatively simple formulas of Ref. 2 for the electrical conductivity and the bootstrap current coefficients, and will be completely presented in the next section and shown in Fig. 5, for all the perpendicular transport coefficients. Hence the study of the effects of plasma shape on the neoclassical transport can be simply obtained considering the dependence of the trapped fraction on plasma elongation and triangularity at a given aspect ratio. Both the two given expressions for the trapped fraction, f_t and f_t^d, Eq. (17), turn out to be almost independent of elongation, and increasing when decreasing triangularity. In this sense, in the neoclassical transport, at a given value of the aspect ratio, a highly triangular plasma shape is favorable for confinement, as shown in Figs. 2(b) and 4(a) (symbol $\triangleright$), but not favorable for driving bootstrap current.

IV. TRANSPORT COEFFICIENTS FORMULAS

A. Analytical fits to the numerical results for the banana regime

Considering the results of the previous section, we can introduce a set of dimensionless electron and ion transport coefficients $\mathcal{K}^\sigma_{mn}$

$$\mathcal{L}^e_{nm}=\mathcal{L}_d[B_0^2\langle B^{-2}\rangle]\mathcal{K}^e_{nm}(f_t^d), \quad n,m=1,2, \tag{20a}$$

$$\mathcal{L}^e_{n3}=\mathcal{L}_b\mathcal{K}^e_{n3}(f_t), \quad n=1,2,4, \tag{20b}$$

$$\mathcal{L}^e_{n4}=\mathcal{L}_d[B_0^2\langle B^2\rangle^{-1}]\mathcal{K}^e_{n4}(f_t), \quad n=1,2, \tag{20c}$$

$$\mathcal{L}^e_{33}=\mathcal{L}_\sigma[B_0^{-2}\langle B^2\rangle]\mathcal{K}^e_{33}(f_t), \tag{20d}$$

$$\mathcal{L}^i_{11}=\mathcal{L}^i_\sigma[B_0^{-2}\langle B^2\rangle]\mathcal{K}^i_{11}(f_t), \tag{20e}$$

$$\mathcal{L}^i_{12}=\mathcal{L}^i_b\mathcal{K}^i_{12}(f_t), \tag{20f}$$

$$\mathcal{L}^i_{22}=\mathcal{L}^i_d[B_0^2\langle B^{-2}\rangle]\mathcal{K}^i_{22}(f_t^d), \tag{20g}$$

and analogously all their symmetrics, where $\mathcal{L}_d$, $\mathcal{L}_b$, and $\mathcal{L}_\sigma$ are defined by Eq. (16); the ion normalization factors, $\mathcal{L}^i_d$, $\mathcal{L}^i_b$, and $\mathcal{L}^i_\sigma$, are defined as follows:

$$\mathcal{L}^i_d=\frac{n_i\rho_{ip}^2}{\tau_i}\left(\frac{d\psi}{d\rho}\right)^2, \quad \mathcal{L}^i_b=I(\psi)n_i, \quad \mathcal{L}^i_\sigma=\frac{n_i q_i^2\tau_i}{m_i T_i}B_0^2. \tag{21}$$

The dimensionless coefficients are functions of only one suitable geometrical parameter, i.e., a trapped fraction, which completely encapsulates the effects of the various equilibria: in this way the code results for the coefficients $\mathcal{K}^\sigma_{mn}$ can be fitted in terms of the appropriate trapped fraction, f_t or f_t^d, as they perfectly overlap, regardless the equilibrium considered in the calculation, even highly noncircular and at small aspect ratio. Note that only in this way relatively simple formulas valid in general axisymmetric equilibria and at all aspect ratios can be given. We have already computed the neoclassical conductivity and the bootstrap current coefficients, in Ref. 2, solving the same kinetic equation of Eq. (13a), $n=3$, and computing the transport coefficients with the same integrals given by Eq. (11), $n=3$, and Eq. (12), $n=2$, $m=1$, which were first obtained using an adjoint formalism[13] adapted to calculate only the bootstrap current: the general kinetic results of Sec. II show, however, that the adjoint formulation is not necessary. The relations between the transport coefficient $\mathcal{L}^e_{33}$ and the neoclassical conductivity σ_{neo}, Eq. (13a) in Ref. 2, and between the dimensionless coefficients $\mathcal{K}^e_{3m}$, $m=1,2,4$, and the bootstrap current coefficients $\mathcal{L}^{bs}_{3m}$, Eqs. (14) and (15) in Ref. 2, read

$$\mathcal{L}^e_{33}=\frac{\sigma_{neo}-\sigma_{Sptz}}{T_e}\langle B^2\rangle, \quad \mathcal{K}^e_{3m}=-\mathcal{L}^{bs}_{3m}. \tag{22}$$

The coefficient $\mathcal{K}^i_{12}$ is related to the coefficient α, Eqs. (17a) and (17b) in Ref. 2, by Eq. (25). [Note: -0.315 should be replaced by $+0.315$ in Eq. (17b).] We have run the code CQL3D with different equilibria and for the electron coefficients we have also varied the ion charge, to obtain the dependence on the effective charge Z. Our idea is that, at least for the electron transport coefficients, an effective charge approximation for multispecies cases should still be valid: collisions between electrons and main ions, or between electrons and impurity ions are almost of the same kind, involving basically the pitch-angle scattering. In any case, the comparison with the results of multispecies codes[8] should enable one to determine the correct form of Z, instead of the usual definition of Z_{eff}, to be used in our formulas, as already mentioned in Ref. 2. For the ions, the presence of one heavy impurity species leads to collisions between main ions and impurity ions which involve basically the pitch-angle scattering, and which are completely different from like–particle collisions. In this case, as shown in Ref. 16, the thermal conductivity computed as Z_{eff} times the pure ion conductivity is underestimated. Using the results of Ref. 16, which uses the large aspect ratio limit of Ref. 17, we have generalized our formula for the transport coefficient $\mathcal{L}^i_{22}$, to include the effect of a single heavy impurity species in the Pfirsch–Schlüter regime. We have also adapted the formula for the bootstrap current coefficient α in the banana regime, Eq. (17a) in Ref. 2, to include the same effect, using the large aspect ratio limit of Ref. 17, and noting that at $\epsilon=1$ not only the pure plasma coefficient, but also the impurity contribution must be equal to zero. The analytical fits to the results of CQL3D for all the transport coefficients not already computed in Ref. 2, valid in the banana regime, for arbitrary trapped fraction and Z, and the modified formula for the bootstrap current coefficient α, read as follows:

$$\mathcal{K}^e_{11}(f_t^d)=-0.5F_{11}(f_t^d), \tag{23a}$$

$$\mathcal{K}^e_{12}(f_t^d)=0.75F_{12}(f_t^d), \tag{23b}$$

$$\mathcal{K}^e_{14}(f_t)=\mathcal{K}^e_{44}=-0.5F_{11}(f_t), \tag{23c}$$

$$\mathcal{K}^e_{22}(f_t^d)=-\left(\frac{13}{8}+\frac{\sqrt{2}}{2Z}\right)F_{22}(f_t^d), \tag{23d}$$

$$\mathcal{K}^e_{24}(f_t)=0.75F_{12}(f_t), \tag{23e}$$

$$\mathcal{K}^i_{22}(f_t^d)=-F^i_{22}(f_t^d), \tag{23f}$$

$$F_{11}(X)\doteq\left(1+\frac{0.9}{Z+0.5}\right)X-\frac{1.9}{Z+0.5}X^2+\frac{1.6}{Z+0.5}X^3-\frac{0.6}{Z+0.5}X^4, \tag{24a}$$

$$F_{12}(X)\doteq\left(1+\frac{0.6}{Z+0.5}\right)X-\frac{0.95}{Z+0.5}X^2+\frac{0.3}{Z+0.5}X^3+\frac{0.05}{Z+0.5}X^4, \tag{24b}$$

$$F_{22}(X)\doteq\left(1-\frac{0.11}{Z+0.5}\right)X+\frac{0.08}{Z+0.5}X^2+\frac{0.03}{Z+0.5}X^3, \tag{24c}$$

$$F^i_{22}(X)\doteq(1-0.55)(1+1.54\alpha_I)X+(0.75X^2-0.7X^3+0.5X^4)(1+2.92\alpha_I), \tag{24d}$$

$$\alpha(f_t)=-\mathcal{K}^i_{12}=-\frac{0.62+1.5\alpha_I}{0.53+\alpha_I}\frac{1-f_t}{1-0.22f_t-0.19f_t^2}, \tag{25}$$

where $\alpha_I=n_IZ_I^2/n_iZ_i^2$ is the usual impurity strength parameter, and index I refers to the ion impurity species. The factorizations used in Eqs. (23) and (24) are such that the Lorentz limit ($Z\to\infty$), the low ($f_t\to0$) and the large aspect ratio ($f_t\to1$) are easily recovered. Moreover the functions F_{ij} have values within [0,1]. Note that $\mathcal{K}^e_{11}$ and $\mathcal{K}^e_{14}$, as well as $\mathcal{K}^e_{12}$ and $\mathcal{K}^e_{24}$ have the same functional dependence on their respective trapped fraction. These relations can be considered as the extension to a general axisymmetric equilibrium at all aspect ratios of Eqs. (6.28)–(6.30) and Eq. (6.47) in Ref. 3. We have also computed the coefficient $\mathcal{L}^i_{11}$, which is usually not considered, following the weak-coupling approximation, which neglects the force A_{i1}. For completeness, we give also the fit to the code results for the transport coefficient $\mathcal{K}^i_{11}$

$$\mathcal{K}^i_{11}(f_t)=(0.11+1.7f_t-1.25f_t^2+0.44f_t^3)^{-1}-1.$$

Note that Eq. (2) allows to reduce the number of independent thermodynamic forces from 6 to 4, hence with only 4 conjugated thermodynamic fluxes. Taking the first 3 electron forces and the second ion force, whose conjugated fluxes have more direct physical meaning and more direct application in the fluid transport equations, the relations which connect fluxes with forces read as follows:

$$B_{en}=\sum_{m=1}^{3}\left\{\mathcal{L}^e_{nm}-\frac{1}{\mathcal{F}}\frac{T_i}{Z_i^2T_e}\frac{\mathcal{L}^i_{11}\mathcal{L}^e_{n4}}{[I(\psi)n_i]^2}\right\}A_{em} - \frac{1}{\mathcal{F}}\frac{T_i}{Z_iT_e}\mathcal{L}^e_{n4}\frac{\mathcal{L}^i_{12}}{I(\psi)n_i}A_{i2}, \quad n=1,2,3, \tag{26a}$$

$$B_{i2}=\frac{1}{\mathcal{F}}\frac{\mathcal{L}^i_{21}}{I(\psi)n_i}\sum_{m=1}^{3}\mathcal{L}^e_{4m}A_{em} + \left\{\mathcal{L}^i_{22}-\frac{1}{\mathcal{F}}\frac{T_i}{Z_i^2T_e}\frac{\mathcal{L}^i_{12}\mathcal{L}^i_{21}}{[I(\psi)n_i]^2}\mathcal{L}^e_{44}\right\}A_{i2}, \tag{26b}$$

where

$$\mathcal{F}\doteq 1+\frac{T_i}{Z_1^2T_e}\frac{\mathcal{L}^i_{11}\mathcal{L}^e_{44}}{[I(\psi)n_i]^2},$$

and Z_i is the main ion charge number. The condition for the validity of the weak-coupling approximation is given by Eq. (5.86) in Ref. 3, and is simply $\mathcal{F}-1\ll 1$. Introducing the dimensionless coefficients $\mathcal{K}^\sigma_{mn}$, this relation reads, consistently with the estimate given in Ref. 3, Table IV

$$\frac{2\sqrt{2}}{Z_i}\left(\frac{m_e}{m_i}\right)^{1/2}\left(\frac{T_i}{T_e}\right)^{3/2}\mathcal{K}^e_{14}\mathcal{K}^i_{11}\ll 1. \tag{27}$$

The absolute value of the term $\mathcal{K}^e_{14}\mathcal{K}^i_{11}$ turns out to be smaller then 0.25, which confirms the validity of the weak coupling approximation in the banana regime. In this way Eq. (26) are reduced to:

$$B_{en}=\sum_{m=1}^{3}\mathcal{L}^e_{nm}A_{em}-\frac{T_i}{Z_iT_e}\mathcal{L}^e_{n4}\frac{\mathcal{L}^i_{12}}{I(\psi)n_i}A_{i2}, \quad n=1,2,3, \tag{28a}$$

$$B_{i2}=\frac{\mathcal{L}^i_{21}}{I(\psi)n_i}\sum_{m=1}^{3}\mathcal{L}^e_{4m}A_{em} + \left\{\mathcal{L}^i_{22}-\frac{T_i}{Z_i^2T_e}\frac{\mathcal{L}^i_{12}\mathcal{L}^i_{21}}{[I(\psi)n_i]^2}\mathcal{L}^e_{44}\right\}A_{i2}. \tag{28b}$$

In Fig. 5 we compare the code results for the dimensionless transport coefficients $\mathcal{K}^\sigma_{nm}$ (symbols) with the algebraic formulas, Eqs. (23) and (24), which fit the data, (solid lines).

B. Combined formulas for all collisionality regimes

In order to compute the neoclassical transport coefficients at arbitrary collisionality regime, the nonbounce-averaged kinetic equations, Eqs. (9) and (10), must be solved. This, as already mentioned, has been done in Ref. 2, to compute the neoclassical resitivity and all the bootstrap current coefficients, using the code CQLP, which includes the advection parallel to the magnetic field, without any assumption on the ratio between the collision frequency and the bounce frequency. In order to strictly compare only the dependence on collisionality, in Fig. 6 we have plotted formulas of Ref. 2 (solid lines) and those of Ref. 3, Sec. VI F (dashed lines), in which we have replaced the banana limit with the correct results of the code CQL3D. The neoclassical resistivity is shown in Fig. 6(a) and the bootstrap current coefficient $\mathcal{L}^e_{31}$ in Fig. 6(b), for three values of the trapped fraction. At low aspect ratio there is a very good agreement, which falls down at larger values of the trapped fraction. This comes from the main approximation adopted to compute the banana-plateau regime, in Ref. 18, which neglects the energy scattering in the like-particle collision operator and which underestimates the neoclassical transport at low aspect ratio.[7] However, for both the neoclassical resistivity and the bootstrap current coefficient $\mathcal{L}^e_{31}$, and also for the coefficient $\mathcal{L}^e_{32}$ not shown here, the Ref. 3 formulas go down to zero at smaller values of ν_{e*} with respect to the rigorous results of Ref. 2, with approximately the same behavior. When the collisional parameter $\nu_{\sigma*}$, defined in Ref. 2, Eq. (18), is rescaled in terms of the trapped fraction with the simple transformation

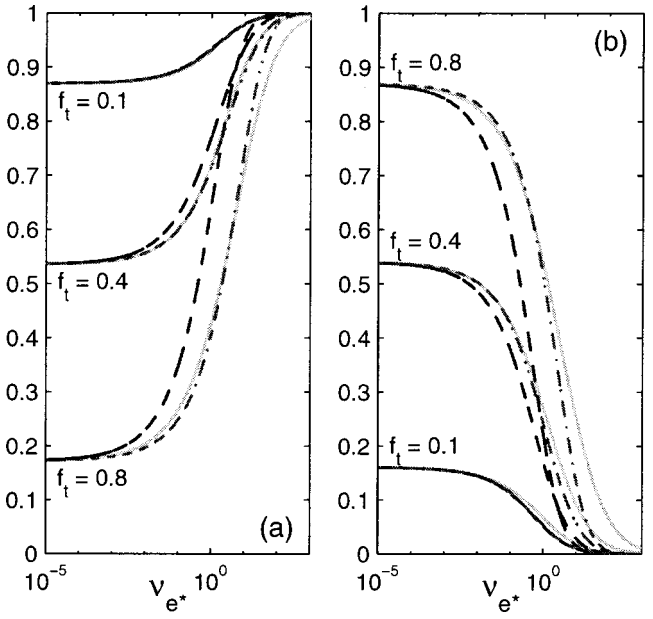

FIG. 6. Dependence on collisionality for the transport coefficients $\sigma_{\rm neo}$, (a) and $\mathcal{L}^e_{31}$, (b), for different values of the trapped fraction f_t, as given by Ref. 1 (solid lines), by Ref. 12, with the value at $\nu_{e*}=0$, banana limit, corrected with the results of Ref. 1 (dashed lines), and still by Ref. 12, with also the collisional parameter rescaled by Eq. (29) (dashed–dotted lines).

$$\nu_{\sigma f*}=\frac{\nu_{\sigma*}}{1+7f_t^2}, \tag{29}$$

Ref. 3 formulas allow an agreement within 20% for all the bootstrap current coefficients and the neoclassical resistivity (dashed–dotted lines), comparing with Ref. 2. Hence, following the idea of Ref. 5, in which a formula valid for all collisionality regimes for the ion heat conductivity is obtained connecting a new banana limit, valid also at small aspect ratio, with the collisional dependence of Ref. 3, we propose to combine formulas of Ref. 3, Sec. VI F, adapted to

small aspect ratio, with the results of this paper in the limit at $\nu_{\sigma *}=0$. The electron transport coefficients $\mathcal{K}^e_{mn}$, $m,n=1,2$ can be computed at arbitrary collisionality regimes as follows:

$$\mathcal{K}^e_{11}(f_t^d,\nu_{e*})=\mathcal{H}^e_{11},\quad \mathcal{K}^e_{12}(f_t^d,\nu_{e*})=\mathcal{H}^e_{12}-\tfrac{5}{2}\mathcal{H}^e_{11},$$
$$\mathcal{K}^e_{22}(f_t^d,\nu_{e*})=\mathcal{H}^e_{22}-5\mathcal{H}^e_{12}+\tfrac{25}{4}\mathcal{H}^e_{11}, \tag{30a}$$

$$\mathcal{H}^e_{mn}(f_t^d,\nu_{e*})=\frac{\mathcal{H}^{e(0)}_{mn}(f_t^d,\nu_{e*}=0)}{1+a_{mn}(Z)\nu_{ef*}^{1/2}+b_{mn}(Z)\nu_{ef*}} - \frac{d_{mn}(Z)\nu_{ef*}f_t^{d^3}(1+f_t^{d^6})}{1+c_{mn}(Z)\nu_{ef*}f_t^{d^3}(1+f_t^{d^6})}F_{PS}, \tag{30b}$$

where the banana limit coefficients $\mathcal{H}^{e(0)}_{mn}(f_t^d,\nu_{e*}=0)$ can be readily evaluated using Eqs. (23) and (24), with

$$\mathcal{H}^{e(0)}_{11}=\mathcal{K}^e_{11}(f_t^d),\quad \mathcal{H}^{e(0)}_{12}=\mathcal{K}^e_{12}(f_t^d)+\tfrac{5}{2}\mathcal{K}^e_{11}(f_t^d),$$
$$\mathcal{H}^{e(0)}_{22}=\mathcal{K}^e_{22}(f_t^d)+5\mathcal{K}^e_{12}(f_t^d)-\tfrac{25}{4}\mathcal{K}^e_{11}(f_t^d). \tag{30c}$$

The coefficients $\mathcal{K}^e_{4n}$ are given by

$$\mathcal{K}^e_{41}(f_t,\nu_{e*})=\mathcal{H}^e_{41},\quad \mathcal{K}^e_{42}(f_t,\nu_{e*})=\mathcal{H}^e_{42}-\tfrac{5}{2}\mathcal{H}^e_{41}, \tag{30d}$$

$$\mathcal{H}^e_{4n}(f_t,\nu_{e*})=\left[\frac{\mathcal{H}^{e(0)}_{4n}(f_t,\nu_{e*}=0)}{1+a_{1n}(Z)\nu_{ef*}^{1/2}+b_{1n}(Z)\nu_{ef*}} - \frac{d_{1n}(Z)\nu_{ef*}f_t^3(1+0.8f_t^3)}{1+c_{1n}(Z)\nu_{ef*}f_t^3(1+0.8f_t^3)}F^{(4)}_{PS}\right] \times\frac{1}{1+\nu^2_{ef*}f_t^{12}} \tag{30e}$$

where analogously

$$\mathcal{H}^{e(0)}_{41}=\mathcal{K}^e_{41}(f_t),\quad \mathcal{H}^{e(0)}_{42}=\mathcal{K}^e_{42}(f_t)+\tfrac{5}{2}\mathcal{K}^e_{41}(f_t), \tag{30f}$$

and with

$$F_{PS}=1-\frac{1}{\langle B^2\rangle\langle B^{-2}\rangle},\quad F^{(4)}_{PS}=\langle B^{-2}\rangle\langle B^2\rangle-1. \tag{30g}$$

The ion thermal conductivity $\mathcal{K}^i_{22}$ is given by

$$\mathcal{K}^i_{22}(f_t^d,\nu_{i*})=\frac{\mathcal{K}^i_{22}(f_t^d)}{1+a_2\mu_{if*}^{1/2}+b_2\mu_{if*}} - \frac{d_2\mu_{if*}f_t^{d^3}(1+f_t^{d^6})}{1+c_2\mu_{if*}f_t^{d^3}(1+f_t^{d^6})}H_PF_{PS}, \tag{30h}$$

with[16] $\mu_{if*}=\nu_{if*}(1+1.54\alpha_I)$ and $H_P=1+1.33\alpha_I(1+0.60\alpha_I)/(1+1.79\alpha_I)$. The coefficients $a_{mn}(Z)$, $b_{mn}(Z)$, $c_{mn}(Z)$, and $d_{mn}(Z)$ are given in Appendix B, obtained by interpolation of the data given in Ref. 3, Table III for the electron coefficients and below Eq. (6.133) for the ion coefficient. The dependence on ϵ of the plateau-collisional terms of the formulas of Ref. 3, first computed in Ref. 19, has been rescaled on f_t or f_t^d. Finite aspect ratio effects in these terms have been taken into account, like in Ref. 5, introducing the complete expression of the Pfirsch–Schlüter geometrical factor, by means of F_{PS} and $F^{(4)}_{PS}$, Eq. (30g). Note that Eq. (30h) for the ion thermal conductivity $\mathcal{K}^i_{22}$ includes the effects of a single heavy impurity species in the Pfirsch–Schlüter regime, according to Ref. 16, using the modified ion collisionality parameter μ_{if*} and the factor H_P, which take into account the enhancement of main ion thermal transport due to the presence of the impurity species.[16]

V. CONCLUSION

We have presented an approach for the neoclassical transport theory which allows to obtain simple equations suited for implementation in numerical codes in order to compute all the neoclassical transport coefficients. The code CQL3D, solving the bounce-averaged linearized drift-kinetic Fokker–Planck equation with the full collision operator, has been modified to calculate all these coefficients at all aspect ratios of various axisymmetric equilibria in the banana regime. We have shown that the limits at large and unit aspect ratio are correctly respected by the numerical results, as also the Onsager symmetry of the nondiagonal transport coefficients. Investigating the dependence of the coefficients on geometry parameters, we have shown that appropriate definitions of trapped fractions are required in order to encapsulate all the geometry effects in a single variable. In this way, a set of simple formulas can be obtained from the numerical results and allow the evaluation of any transport coefficient for every axisymmetric equilibrium and at all aspect ratios. Our formula for the ion thermal conductivity is in good agreement with the most recent evaluations of this coefficient,[5,6] which, however, do not use the full collision operator, with errors at finite aspect ratio of about 10% by excess and by defect, respectively. For all the other perpendicular transport coefficients, in particular the electron thermal conductivity, our formulas are the only existing to date and to our knowledge, computed for general axisymmetric equilibria taking into account finite aspect ratio effects. The transport coefficients formulas, which fit the numerical results in the banana regime, are given by Eqs. (20)–(24) of Sec. IV A. Extension of this work is to compute the transport coefficients at all collisionality regimes: note that this has already been done for the neoclassical conductivity and the bootstrap current coefficients in Ref. 2. These results, compared with the ones of Refs. 3 and 5, have motivated us to propose combined formulas for all the other transport coefficients, valid for arbitrary collisionality regime, needed to correctly evaluate these coefficients over the whole plasma minor radius. The thermodynamic fluxes

$$B_{e1}=\Gamma_e\frac{d\psi}{d\rho},\quad B_{e2}=\frac{Q_e}{T_e}\frac{d\psi}{d\rho},$$
$$B_{e3}=\frac{\langle j_\parallel B\rangle}{T_e}-\frac{\langle j_{\parallel S}B\rangle}{T_e},\quad B_{i2}=\frac{Q_i}{T_i}\frac{d\psi}{d\rho},$$

where Γ_e is the perpendicular electron particle flux, Q_e is the electron perpendicular heat flux, $j_\parallel$ and $j_{\parallel S}$ are the parallel electric current and the Spitzer current, and Q_i is the ion perpendicular heat flux, are given by Eqs. (28), in the weak coupling approximation, whose validity is confirmed by Eq. (27). Equations (28) can be reordered, and the thermody-

namic fluxes can be expressed directly in terms of the electron and ion temperature and density perpendicular gradients and the parallel electric field

$$B_{en}=\mathcal{L}^e_{n1}\frac{\partial \ln n_e}{\partial\psi}+(\mathcal{L}^e_{n1}+\mathcal{L}^e_{n2})\frac{\partial \ln T_e}{\partial\psi}+\frac{1-R_{pe}}{R_{pe}}\mathcal{L}^e_{n1}\frac{\partial \ln n_i}{\partial\psi}+\frac{1-R_{pe}}{R_{pe}}(\mathcal{L}^e_{n1}+\alpha\mathcal{L}^e_{n4})\times\frac{\partial \ln T_i}{\partial\psi}+\mathcal{L}^e_{n3}\frac{\langle E_\parallel B\rangle}{\langle B^2\rangle},\quad n=1,2,3,$$

$$B_{i2}=\frac{Q_i}{T_i}\frac{d\psi}{d\rho}=\alpha\Bigg[\mathcal{L}^e_{41}\frac{\partial \ln n_e}{\partial\psi}+(\mathcal{L}^e_{41}+\mathcal{L}^e_{42})\frac{\partial \ln T_e}{\partial\psi}+\mathcal{L}^e_{41}\frac{1-R_{pe}}{R_{pe}}\frac{\partial \ln n_i}{\partial\psi}+\mathcal{L}^e_{43}\frac{\langle E_\parallel B\rangle}{\langle B\rangle^2}+\left(\mathcal{L}^i_{22}+\frac{1-R_{pe}}{R_{pe}}\frac{\alpha^2}{Z_i}\mathcal{L}^e_{44}\right)\frac{\partial \ln T_i}{\partial\psi},$$

where $R_{pe}\doteq p_e/p$ and Z_i is the main ion charge number. The perpendicular transport coefficients $\mathcal{L}^\sigma_{mn}$, for general axisymmetric equilibria and arbitrary collisionality regime, are given by Eqs. (30) of Sec. IV B in terms of the trapped fractions f_t or f^d_t, Eq. (17), the collisionality parameter ν_* and the effective charge number Z. The neoclassical conductivity and the bootstrap current coefficients, $\mathcal{L}^e_{3n}$ and α, are connected with formulas of Ref. 2 by Eqs. (22) and (25).

ACKNOWLEDGMENTS

We are grateful to Y.R. Lin-Liu and J. Vaclavik for interesting discussions. One of the authors, C.A., would also like to thank P. Helander for useful discussions. This work was partly supported by the Swiss National Science Foundation.

APPENDIX A: ONSAGER SYMMETRY OF THE TRANSPORT COEFFICIENTS

The expressions for the transport coefficients given by Eq. (11) for the electrons and by Eq. (12) for the ions satisfy the Onsager relations of symmetry, as expected.[3] We begin with the electron case. In Eq. (11), the first term, $\mathcal{L}^{e(1)}_{mn}\doteq\langle\int d\mathbf{v}\gamma_{em}C^l_{e0}(\gamma_{en}f_{e0})\rangle$, is symmetric directly from the self-adjointness of the collision operator. Hence

$$\mathcal{L}^{e(1)}_{mn}\doteq\left\langle\int d\mathbf{v}\gamma_{em}C^l_{e0}(\gamma_{en}f_{e0})\right\rangle=\left\langle\int d\mathbf{v}\gamma_{en}C^l_{e0}(\gamma_{em}f_{e0})\right\rangle\doteq\mathcal{L}^{e(1)}_{nm}. \tag{A1}$$

For the second term, $\mathcal{L}^{e(2)}_{mn}\doteq\langle\int d\mathbf{v}g_{em}/f_{e0}C^l_{e0}(\gamma_{en}f_{e0})\rangle$, we shall rewrite it in a symmetric form. Introducing the following notation,[3] for a generic function $f(\mathbf{v})$, $f^+\doteq\frac{1}{2}[f(\sigma=+1)+f(\sigma=-1)]$ is its even part in $\sigma=v_\parallel/|v_\parallel|$ and $f^-\doteq\frac{1}{2}[f(\sigma=+1)-f(\sigma=-1)]$ is the odd part, so that

$$|v_\parallel|\hat{\mathbf{b}}\cdot\nabla g^+_{en}-C^l_{e0}(g^-_{en})=-C^l_{e0}(\gamma_{en}f_{e0}),$$
$$|v_\parallel|\hat{\mathbf{b}}\cdot\nabla g^-_{en}-C^l_{e0}(g^+_{en})=0 \tag{A2}$$

[as $C^l_{e0}(\gamma_{en}f_{e0})^-=C^l_{e0}(\gamma_{en}f_{e0})$ and $C^l_{e0}(\gamma_{en}f_{e0})^+=0$, $n=1,2,3,4$]
we can perform the following derivation:

$$\begin{aligned}\mathcal{L}^{e(2)}_{mn}&\doteq\left\langle\int d\mathbf{v}\frac{g_{em}}{f_{e0}}C^l_{e0}(\gamma_{en}f_{e0})\right\rangle\\&=\left\langle\int d\mathbf{v}\frac{g^-_{em}}{f_{e0}}C^l_{e0}(\gamma_{en}f_{e0})^-\right\rangle\\&=-\left\langle\int d\mathbf{v}\frac{g^-_{em}}{f_{e0}}[v_\parallel\hat{\mathbf{b}}\cdot\nabla g^+_{en}-C^l_{e0}(g^-_{en})]\right\rangle\\&=-\left\langle\int d\mathbf{v}\frac{1}{f_{e0}}[-g^+_{em}|v_\parallel|\hat{\mathbf{b}}\cdot\nabla g^-_{en}-g^-_{em}C^l_{e0}(g^-_{en})]\right\rangle\\&=-\left\langle\int d\mathbf{v}\frac{1}{f_{e0}}[-g^+_{em}C^l_{e0}(g^+_{en})-g^-_{em}C^l_{e0}(g^-_{en})]\right\rangle\\&=\left\langle\int d\mathbf{v}\frac{1}{f_{e0}}g_{em}C^l_{e0}(g_{en})\right\rangle,\end{aligned}$$

which is a symmetric expression, using the self-adjointness of the collision operator. (Note that we have used in this derivation the fact that the operator $-v_\parallel\hat{\mathbf{b}}\cdot\nabla$ is the adjoint of the operator $v_\parallel\hat{\mathbf{b}}\cdot\nabla$.) Hence we can conclude that

$$\mathcal{L}^{e(2)}_{mn}=\left\langle\int d\mathbf{v}\frac{1}{f_{e0}}g_{em}C^l_{e0}(g_{en})\right\rangle=\left\langle\int d\mathbf{v}\frac{1}{f_{e0}}g_{en}C^l_{e0}(g_{em})\right\rangle=\mathcal{L}^{e(2)}_{nm}, \tag{A3}$$

which shows the symmetry of the coefficients $\mathcal{L}^e_{mn}$. A somewhat analogous calculation can be performed for the ion coefficients $\mathcal{L}^i_{12}$ and $\mathcal{L}^i_{21}$, which shows that the two given expressions, Eq. (12), satisfy the following relation:

$$\mathcal{L}^i_{12}=-\mathcal{L}^i_{21}, \tag{A4}$$

consistently with the result in Ref. 3, Eq. (5.99).

APPENDIX B: COEFFICIENTS FOR THE COMBINED FORMULAS OF SEC. IV B

The coefficients $a_{mn}(Z)$, $b_{mn}(Z)$, $c_{mn}(Z)$, and $d_{mn}(Z)$ for the electron transport coefficients are defined as follows:

$$a_{11}(Z)=\frac{1+3Z}{0.77+1.22Z},\qquad a_{12}(Z)=\frac{0.72+0.42Z}{1+0.5Z},\quad a_{22}(Z)=0.46, \tag{B1a}$$

$$b_{11}(Z)=\frac{1+1.1Z}{1.37Z},\quad b_{12}(Z)=\frac{1+Z}{2.99Z},\qquad b_{22}(Z)=\frac{Z}{-3+5.32Z}, \tag{B1b}$$

$$c_{11}(Z)=\frac{0.1+0.34Z}{1.65Z},\quad c_{12}(Z)=\frac{0.27+0.4Z}{1+3Z},$$
$$c_{22}(Z)=\frac{0.22+0.55Z}{-1+7Z}, \tag{B1c}$$

$$d_{11}(Z)=\frac{0.23Z}{-1+3.85Z},$$
$$d_{12}(Z)=\frac{0.22+0.38Z}{1+6.1Z},\quad d_{22}(Z)=\frac{0.25+0.05Z}{1+0.82Z}. \tag{B1d}$$

For the ion thermal conductivity, the coefficients are

$$a_2=1.03,\quad b_2=0.31,\quad c_2=0.22,\quad d_2=0.175. \tag{B2}$$

[1]O. Sauter, C. Angioni, and Y. R. Lin-Liu, Phys. Plasmas **6**, 2834 (1999).
[2]S. P. Hirshman and D. J. Sigmar, Nucl. Fusion **21**, 1079 (1981).
[3]C. S. Chang and F. L. Hinton, Phys. Fluids **25**, 1493 (1982).
[4]M. Taguchi, Plasma Phys. Controlled Fusion **30**, 1897 (1988).
[5]C. Bolton and A. A. Ware, Phys. Fluids **26**, 459 (1983).
[6]W. A. Houlberg, K. C. Shaing, S. P. Hirshman, and M. C. Zarnstorff, Phys. Plasmas **4**, 3230 (1997).
[7]S. P. Hirshman and D. J. Sigmar, Phys. Fluids **19**, 1532 (1976).
[8]S. P. Hirshman, Phys. Fluids **31**, 3150 (1988).
[9]R. D. Hazeltine, F. L. Hinton, and M. N. Rosenbluth, Phys. Fluids **16**, 1645 (1973).
[10]M. N. Rosenbluth, R. D. Hazeltine, and F. L. Hinton, Phys. Fluids **15**, 116 (1972).
[11]R. W. Harvey and M. G. McCoy, in *Proceedings of International Atomic Energy Agency Technical Committee Meeting on Advances in Simulation and Modeling of Thermonuclear Plasmas, Montreal, 1992* (International Atomic Energy Agency, Vienna, 1993), pp. 489–526; J. Killeen, G. D. Kerbel, M. G. McCoy, and A. A. Mirin, *Computational Methods for Kinetic Models of Magnetically Confined Plasmas* (Springer-Verlag, New York, 1986).
[12]F. L. Hinton and R. D. Hazeltine, Rev. Mod. Phys. **48**, 239 (1976).
[13]Y. R. Lin-Liu, private communication (see Ref. 29 in Ref. 8).
[14]P. H. Rutherford, Phys. Fluids **13**, 482 (1970).
[15]Y. R. Lin-Liu and R. L. Miller, Phys. Plasmas **2**, 1666 (1995).
[16]C. S. Chang and F. L. Hinton, Phys. Fluids **29**, 1493 (1986).
[17]S. P. Hirshman, Phys. Fluids **19**, 155 (1976).
[18]F. L. Hinton and M. N. Rosenbluth, Phys. Fluids **16**, 836 (1973).
[19]J. M. Rawls, M. S. Chu, and F. L. Hinton, Phys. Fluids **18**, 1160 (1975).